

## Experimental overview on hadronic resonance production in high-energy nuclear collisions

This content has been downloaded from IOPscience. Please scroll down to see the full text.

2017 J. Phys.: Conf. Ser. 779 012018

(<http://iopscience.iop.org/1742-6596/779/1/012018>)

View [the table of contents for this issue](#), or go to the [journal homepage](#) for more

Download details:

IP Address: 131.169.5.251

This content was downloaded on 13/02/2017 at 20:50

Please note that [terms and conditions apply](#).

You may also be interested in:

[Experimental Overview of Open Heavy Flavor](#)

Kai Schweda

[Heavy flavours in high-energy nuclear collisions: quenching, flow and correlations](#)

A Beraudo, A De Pace, M Monteno et al.

[Partonic collectivity in high-energy nuclear collisions](#)

Nu Xu

[Fluctuations of Conserved Quantities in High Energy Nuclear Collisions at RHIC](#)

Xiaofeng Luo

[Blast wave fits with resonances to pt spectra from nuclear collisions at the LHC](#)

Ivan Melo and Boris Tomášik

[Statistical production of pentaquarks in high-energy nuclear collisions](#)

Jørgen Randrup

[Status of High-Energy Neutrino Astronomy](#)

Marek Kowalski

[Partonic EoS in high-energy nuclear collisions at RHIC](#)

Nu Xu

[Hadronic matter phases and their application to rapidly rotating neutron stars](#)

Tomoki Endo

# Experimental overview on hadronic resonance production in high-energy nuclear collisions

Yosuke Watanabe

Center for Nuclear Study, the University of Tokyo

E-mail: wyosuke@cns.s.u-tokyo.ac.jp

**Abstract.** I summarize recent results of low-mass vector meson measurements in high-energy nuclear collisions.

## 1. Introduction

Hadronic resonances are important tools to study the properties of the hot and dense medium created in high-energy nuclear collisions. Table 1 summarizes the properties of low-mass vector mesons discussed in this article,  $\rho$ ,  $\omega$ ,  $\phi$  and  $K^*$  [1]. Due to the variations in the lifetimes and the decay modes, these resonances are sensitive to different aspects of the space-time evolution of the medium.

For example, the  $\rho$  meson has a short lifetime of 1.3 fm and is expected to decay inside the hot medium. Dilepton decays of the  $\rho$  meson directly carry the information about its in-medium properties, because leptons do not suffer from final state interactions with the medium. On the other hand, hadronic decays, such as  $\rho \rightarrow \pi^+\pi^-$ , are also sensitive to the later stage of the system evolution through the final state interactions of the daughter particles.

In contrast to the  $\rho$  meson, the  $\phi$  meson has a long lifetime and decays after freezeout of the hot medium. Since the hadronic-interaction cross section of the  $\phi$  meson is small, the  $\phi$  meson is expected to be frozen at an early stage and carry the information from the quark-gluon plasma (QGP).

## 2. Dilepton decays

In the hot and dense medium created in heavy-ion collisions, chiral symmetry is expected to be restored, and consequently, the spectral shapes of low-mass vector mesons could undergo modifications from the shapes in vacuum. Dilepton decays are suitable for the detection of such spectral modifications.

Dilepton measurements in the low-mass region below 1 GeV/ $c^2$  are performed by SPS experiments, such as CERES and NA60 [2–7]. These experiments observed an enhancement from cocktail calculations of known hadronic sources at dilepton invariant mass ( $m_{ll}$ ) around 500 MeV/ $c^2$ . This excess is identified as the contributions from the pion annihilation into dileptons, mediated by the  $\rho$  meson ( $\pi\pi \rightarrow \rho \rightarrow \gamma^* \rightarrow ll$ ), inside the hot medium. Two main approaches are taken to describe the in-medium  $\rho$  spectral shapes: “broadening” and “mass shift”. There seems now to be consensus that the “broadening” models are successful in describing the excess in the invariant mass spectra at SPS energies [8–13].



**Table 1.** Properties of low mass vector mesons [1].

	$\rho$	$\omega$	$\phi$	$K^*$
Mass (MeV/ $c^2$ )	775	783	1019	896
Lifetime (fm/ $c$ )	1.3	23	46	4.2
Decay modes	$l^+l^-$ , $\pi^+\pi^-$	$l^+l^-$	$l^+l^-$ , $K^+K^-$	$K^+\pi^-$

The connection between the  $\rho$  broadening models and the chiral symmetry restoration is currently being studied theoretically. For example, Ref. [14] demonstrates that the broadened  $\rho$  spectra get degenerated with its chiral partner, the  $a_1$  meson, at high temperature, which is an indication of the chiral symmetry restoration.

Many experiments are ongoing to perform further studies of the in-medium  $\rho$  spectral shape at different collision energies. Here, most recent results from PHENIX, STAR, ALICE and HADES are summarized.

### 2.1. RHIC and LHC

At RHIC energies, PHENIX and STAR are performing dielectron measurements at midrapidity in heavy-ion collisions. There used to be discrepancies between PHENIX [15] and STAR [16,17] in Au-Au collisions at  $\sqrt{s_{NN}} = 200$  GeV.

Recently, PHENIX published new dielectron results, which solves the discrepancies. Those new results are obtained with the data sets taken in the 2010 RHIC run [18], in which PHENIX installed a new detector, called hadron-blind detector (HBD), to improve the signal-to-background ratio of the dielectron measurements. The enhancement factor in the mass region 0.3–0.76 GeV/ $c^2$  reported by PHENIX is  $2.3 \pm 0.4(stat) \pm 0.4(syst) \pm 0.2(model)$  [18], which is consistent with  $1.76 \pm 0.06(stat) \pm 0.26(syst) \pm 0.29(model)$  reported by STAR [16,17]. These two results are consistent with each other including the centrality and  $p_T$  dependence of the excess.

The PHENIX and the STAR results are well described by the  $\rho$  broadening models, which were successful at SPS energies. STAR is further studying the excess as a function of collision energy down to  $\sqrt{s_{NN}} = 20$  GeV [19] and also in a heavier system, U-U collisions [20]. Currently, all the available experimental data at RHIC are well described by the same  $\rho$  broadening models.

At this conference, ALICE presented dielectron spectra below  $m_{ll} < 1$  GeV/ $c^2$  in Pb-Pb collisions at  $\sqrt{s_{NN}} = 2.76$  TeV for the first time [21]. Figure 1 shows the dielectron spectrum (blue points) compared to the cocktail calculations of hadronic sources (black solid line) for the 0-10% centrality bin. They are applying single  $p_T$  cut of 0.4 GeV/ $c$ , which is stronger than the cut of 0.2 GeV/ $c$  used by the RHIC experiments. No significant enhancement from the cocktail is observed in the ALICE data, which could be attributed to the large experimental uncertainties and large contributions from heavy-flavor decays. The upper limits on the excess do not contradict with the RHIC experiments and also with the real photon measurements performed by ALICE.

One of the difficulties of dilepton measurements at high energies are in the huge contributions from open-charm semileptonic decays,  $c\bar{c} \rightarrow l^+l^-X$ , as is shown as a magenta line in Fig. 1. The large model dependence of  $c\bar{c}$  calculations is recently discussed by PHENIX [18]. The enhancement factor of the new PHENIX data is  $2.3 \pm 0.4(stat) \pm 0.4(syst) \pm 0.2(model)$  when PYTHIA [22] scaled by  $N_{coll}$  is used for the  $c\bar{c}$  calculation, while the enhancement factor becomes  $1.7 \pm 0.3(stat) \pm 0.3(syst) \pm 0.2(model)$  when MC@NLO [23, 24] is used instead of PYTHIA In

addition, the simple  $N_{coll}$  scaling of PYTHIA or MC@NLO does not take into account the energy loss of charm quarks inside the QGP. Thus, further studies of the  $c\bar{c}$  contribution both in elementary and heavy-ion collisions are essential to define the excess precisely.

## 2.2. HADES

Dielectron spectra at lower energies are systematically studied in various collision systems, such as  $pp$ ,  $p$ -Nb, Ar-KCl and Au-Au, by HADES [25]. Figure 2 shows the excess spectrum in Au-Au collisions at 1.23A GeV presented at this conference. In the figure, the data points are compared to theoretical model calculations both including the in-medium broadening of the  $\rho$  meson [26,27]. These models also describe the dielectron excess in a smaller collision system, Ar-KCl collisions [28].

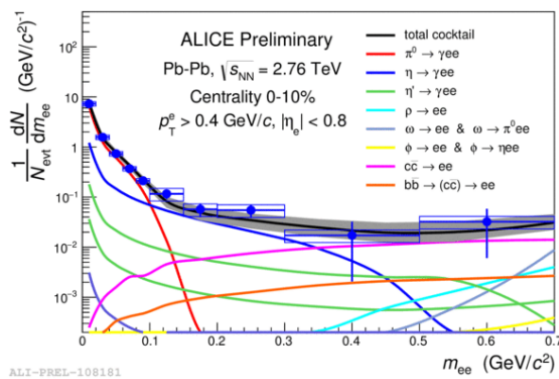


**Figure 1.** Dielectron spectra in the most central Pb-Pb collisions measured by ALICE [21]. The solid lines show the cocktail calculations of hadronic sources.

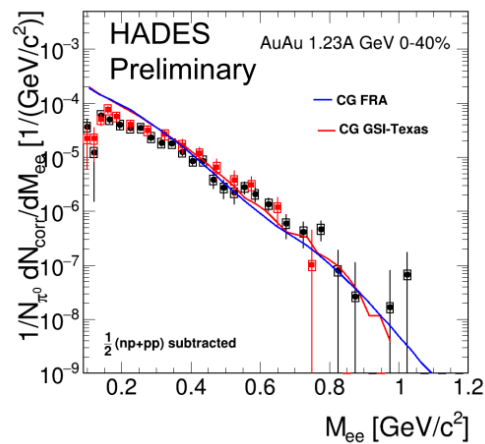


**Figure 2.** Dielectron excess spectra in Au-Au collisions measured by HADES [25]. The data points are compared to the model calculations (solid lines) including the in-medium broadening of the  $\rho$  meson.

## 3. Hadronic decays

The reconstruction of low-mass vector mesons with their hadronic decays is affected not only by the chiral symmetry restoration but also by the final state interactions of daughter particles. Therefore, to understand their spectral shapes and yields, a full description of the medium evolution is required.

The detection of spectral shape modifications using hadronic decays is experimentally challenging. The background contributions in the invariant mass spectra are usually subtracted by fitting the spectra with a combined function describing the background and the signal peak. In this way, the strongly modified signal is indistinguishable from the background. Small modifications can be detected as a change in the signal peak, however, such modifications are not detected, for example, in a  $K^*$  measurement by ALICE [29].

In this section, recent results on the yields of  $\rho$  and  $K^*$  are summarized.

### 3.1. $\rho$ meson

Figure 3 shows the  $\rho \rightarrow \pi^+\pi^-$  invariant mass spectra in Pb-Pb collisions reported by ALICE at this conference [30]. Even in the most central and also in the very low  $p_T$  bin, the  $\rho$  meson

peak is clearly visible.

Figure 4 shows the  $\rho/\pi$  ratio as a function of  $(dN_{ch}/d\eta)^{1/3}$  in  $pp$  and Pb-Pb collisions. The  $\rho/\pi$  ratio is suppressed in central collisions compared to peripheral and  $pp$  collisions. This result indicates that rescattering processes dominate over regeneration processes during the hadronic phase. Figure 4 also shows the EPOS3 calculations with and without UrQMD afterburner, which describes the interactions in the hadronic phase [31]. While EPOS3 without UrQMD is not able to describe the decreasing trend of the data points, EPOS3 with UrQMD qualitatively describes the trend. Thus, the description of the hadronic phase is crucial to understand the measured yields.

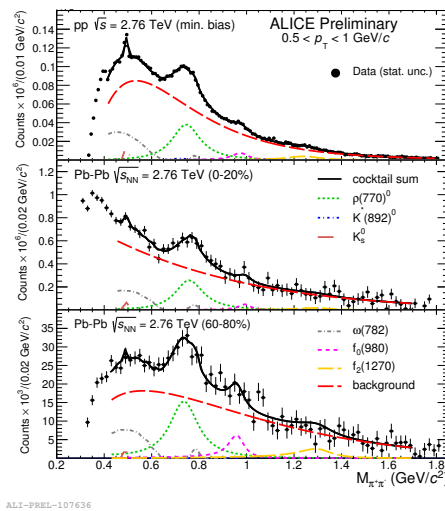


**Figure 3.** The  $\pi^+\pi^-$  invariant mass spectra in  $pp$  (top), in the central Pb-Pb collisions (middle) and in the peripheral Pb-Pb collisions (bottom) measured by ALICE [30].

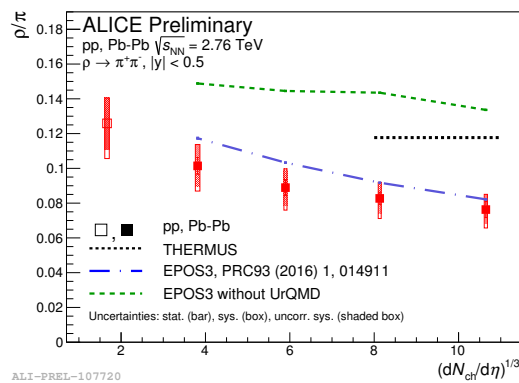


**Figure 4.** The  $\rho/\pi$  ratio as a function of  $(dN_{ch}/d\eta)^{1/3}$  in  $pp$  and Pb-Pb collisions measured by ALICE [30].

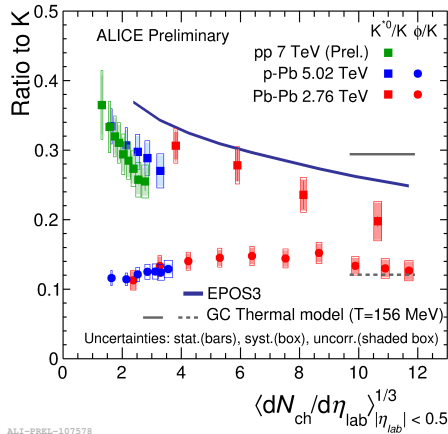
### 3.2. $K^*$ meson

Figure 5 shows the  $K^*/K$  ratio (and the  $\phi/K$  ratio) as a function of  $(dN_{ch}/d\eta)^{1/3}$  in various collisions systems [29, 30, 32, 33]. A similar suppression pattern as the  $\rho/\pi$  ratio is seen for Pb-Pb collisions. The suppression pattern is again qualitatively described by the EPOS3 calculation with the UrQMD afterburner [31].

In the same figure, the multiplicity dependence of the  $K^*/K$  ratio in  $pp$  and  $p$ -Pb collisions is also shown. Similarly to the Pb-Pb collision results, the ratio decreases towards higher multiplicity bins. These results could be suggestive of the presence of rescattering effects even in such small collision systems.

### 4. $\phi$ meson

The  $\phi$  meson is expected to be a penetrating probe of the hadronic phase due to its long lifetime and also due to its small hadronic interaction cross sections. In this section, as an example of the measurements using its penetrating nature, the elliptic flow ( $v_2$ ) measurements by STAR are presented.



**Figure 5.** The  $K^*/K$  ratio as a function of a cube root of  $dN_{ch}/d\eta$  in  $pp$ ,  $p$ -Pb and Pb-Pb collisions measured by ALICE [29, 30, 32, 33].

#### 4.1. Elliptic flow ( $v_2$ )

Hydrodynamical models predict the mass ordering of  $v_2$  at low  $p_T$ , e.g.  $v_2^\pi > v_2^K > v_2^p$ . However, this mass ordering can be broken between proton and the  $\phi$  meson due to large rescattering effects in the hadronic phase only on the proton  $v_2$  [34].

Figure 6 shows the  $\phi$   $v_2$  divided by the proton  $v_2$  as a function of  $p_T$  in Au-Au collisions measured by STAR [35, 36]. Although the  $\phi$  meson is heavier than proton, the ratio is above unity, an indication of violation of the mass ordering, in the  $p_T$  region below 0.5 GeV/c. In the top panel of the figure, the data points are compared to the hydrodynamical model with and without a hadron cascade model (JAM). By taking into account the hadron interactions, the breakdown of the mass ordering is well described by the hydro model.

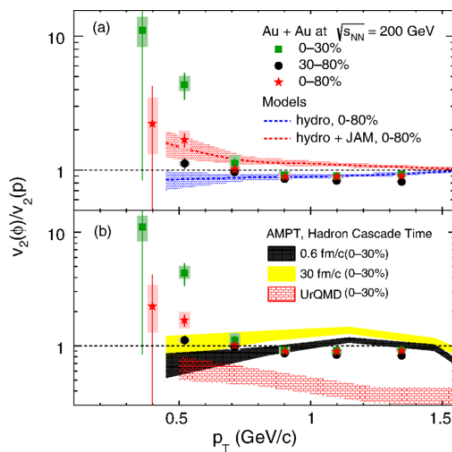


**Figure 6.** The ratio of  $\phi$   $v_2$  and proton  $v_2$  as a function of  $p_T$  for 0-10%, 30-80% and 0-80% centrality bin in Au-Au collisions measured by STAR. The bands in the top and bottom panels show the hydro models and transport model calculations, respectively [35, 36].

## 5. Summary

A broad range of new experimental results on low-mass vector meson measurements is presented at this conference.

Dilepton decays of low-mass vector mesons are studied by various experiments over wide ranges of energies. So far, all the available data sets are well described by theoretical models including the broadening of the  $\rho$  meson. At high energies, the understanding of the open-charm contributions are essential to study the in-medium  $\rho$  spectra in a more precise way.

In hadronic decays, the suppression of the  $K^*$  meson and the  $\rho$  meson are observed in central heavy-ion collisions. These results are indicative of the significant role of the hadronic phase in

the understanding of the resonance production. Similar suppression pattern is also observed in small collision systems, such as  $pp$  and  $p$ -Pb collisions.

Lastly, the breakdown of the mass ordering between proton  $v_2$  and  $\phi$   $v_2$  is observed at top RHIC energies. This result is consistent with a view that the  $\phi$  meson has a small hadronic-interaction cross section and is not strongly affected by the final state interactions with the hadronic medium.

## References

- [1] Olive K A *et al.* (Particle Data Group) 2014 *Chin. Phys.* **C38** 090001
- [2] Agakichiev G *et al.* (CERES) 1995 *Phys. Rev. Lett.* **75** 1272–1275
- [3] Agakishiev G *et al.* (CERES/NA45) 1998 *Phys. Lett.* **B422** 405–412 (*Preprint nucl-ex/9712008*)
- [4] Adamova D *et al.* 2008 *Phys. Lett.* **B666** 425–429 (*Preprint nucl-ex/0611022*)
- [5] Adamova D *et al.* (CERES/NA45) 2003 *Phys. Rev. Lett.* **91** 042301 (*Preprint nucl-ex/0209024*)
- [6] Arnaldi R *et al.* (NA60) 2006 *Phys. Rev. Lett.* **96** 162302 (*Preprint nucl-ex/0605007*)
- [7] Arnaldi R *et al.* (NA60) 2009 *Eur. Phys. J.* **C61** 711–720 (*Preprint 0812.3053*)
- [8] van Hees H and Rapp R 2006 *Phys. Rev. Lett.* **97** 102301 (*Preprint hep-ph/0603084*)
- [9] van Hees H and Rapp R 2008 *Nucl. Phys.* **A806** 339–387 (*Preprint 0711.3444*)
- [10] Ruppert J, Gale C, Renk T, Lichard P and Kapusta J I 2008 *Phys. Rev. Lett.* **100** 162301 (*Preprint 0706.1934*)
- [11] Dusling K, Teaney D and Zahed I 2007 *Phys. Rev.* **C75** 024908 (*Preprint nucl-th/0604071*)
- [12] Bratkovskaya E L, Cassing W and Linnyk O 2009 *Phys. Lett.* **B670** 428–433 (*Preprint 0805.3177*)
- [13] Linnyk O, Bratkovskaya E L, Ozvenchuk V, Cassing W and Ko C M 2011 *Phys. Rev.* **C84** 054917 (*Preprint 1107.3402*)
- [14] Hohler P M and Rapp R 2014 *Phys. Lett.* **B731** 103–109 (*Preprint 1311.2921*)
- [15] Adare A *et al.* (PHENIX) 2010 *Phys. Rev.* **C81** 034911 (*Preprint 0912.0244*)
- [16] Adamczyk L *et al.* (STAR) 2014 *Phys. Rev. Lett.* **113** 022301 (*Preprint 1312.7397*)
- [17] Adamczyk L *et al.* (STAR) 2015 (*Preprint 1504.01317*)
- [18] Adare A *et al.* (PHENIX) 2016 *Phys. Rev.* **C93** 014904 (*Preprint 1509.04667*)
- [19] Ruan L 2014 *Nucl. Phys.* **A931** 185–193 (*Preprint 1407.8153*)
- [20] Yang S (STAR) 2016 *Nucl. Phys.* **A956** 429–432
- [21] See A. Caliva, “Measurement of dielectrons in pp, p–Pb and Pb–Pb collisions with ALICE at the LHC”, in these proceedings
- [22] Sjostrand T, Eden P, Friberg C, Lonnblad L, Miu G, Mrenna S and Norrbin E 2001 *Comput. Phys. Commun.* **135** 238–259 (*Preprint hep-ph/0010017*)
- [23] Frixione S and Webber B R 2002 *JHEP* **06** 029 (*Preprint hep-ph/0204244*)
- [24] Frixione S, Nason P and Webber B R 2003 *JHEP* **08** 007 (*Preprint hep-ph/0305252*)
- [25] See R. Holzmann, “Particle production investigated with HADES at SIS18”, in these proceedings
- [26] Galatyuk T, Hohler P M, Rapp R, Seck F and Stroth J 2016 *Eur. Phys. J.* **A52** 131 (*Preprint 1512.08688*)
- [27] Endres S, van Hees H, Weil J and Bleicher M 2015 *Phys. Rev.* **C92** 014911 (*Preprint 1505.06131*)
- [28] Agakishiev G *et al.* (HADES) 2011 *Phys. Rev.* **C84** 014902 (*Preprint 1103.0876*)
- [29] Abelev B B *et al.* (ALICE) 2015 *Phys. Rev.* **C91** 024609 (*Preprint 1404.0495*)
- [30] See A. Knospe, “Recent Hadronic Resonance Measurements at ALICE”, in these proceedings
- [31] Knospe A G, Markert C, Werner K, Steinheimer J and Bleicher M 2016 *Phys. Rev.* **C93** 014911 (*Preprint 1509.07895*)
- [32] Adam J *et al.* (ALICE) 2016 *Eur. Phys. J.* **C76** 245 (*Preprint 1601.07868*)
- [33] See F. Bellini, “Strangeness in ALICE at LHC”, in these proceedings
- [34] Hirano T, Heinz U W, Kharzeev D, Lacey R and Nara Y 2008 *Phys. Rev.* **C77** 044909 (*Preprint 0710.5795*)
- [35] Adamczyk L *et al.* (STAR) 2016 *Phys. Rev. Lett.* **116** 062301 (*Preprint 1507.05247*)
- [36] See S. Shi, “Strangeness in STAR at RHIC”, in these proceedings